

MIT Open Access Articles

Organic gas emissions from a stoichiometric direct injection spark ignition engine operating on ethanol/gasoline blends

The MIT Faculty has made this article openly available. **Please share** how this access benefits you. Your story matters.

Citation: Kar, K et al. "Organic gas emissions from a stoichiometric direct injection spark ignition engine operating on ethanol/gasoline blends." International Journal of Engine Research 11 (2010): 499-513. Web. 3 Nov. 2011. © 2010 Sage Publications, inc.

As Published: <http://dx.doi.org/10.1243/14680874JER610>

Publisher: Sage Publications, inc.

Persistent URL: <http://hdl.handle.net/1721.1/66909>

Version: Author's final manuscript: final author's manuscript post peer review, without publisher's formatting or copy editing

Terms of use: Creative Commons Attribution-Noncommercial-Share Alike 3.0



Organic Gas Emissions from a Stoichiometric Direct Injection Spark Ignition Engine Operating on Ethanol/ Gasoline Blends

K. Kar, R. Tharp, M. Radovanovic, I. Dimou, and W. K. Cheng*

Sloan Automotive Lab, Massachusetts Institute of Technology

*Corresponding author

Manuscript has figures and captions embedded in text for readability. Final manuscript will have separated figure captions and figures.

ABSTRACT:

The organic gas emissions from a stoichiometric direct injection spark ignition engine operating on ethanol/gasoline blends have been assessed under warmed up and cold idle conditions. The speciated emissions show that the total organic gas emissions (in ppmC1) decrease with increase of ethanol content. The mole fraction of ethanol in the exhaust is proportional to the volume fraction of ethanol in the fuel: 10 percentage points increase in the latter would yield 5.5 percentage point increase in the former. The ethanol to acetaldehyde ratio (by mole) in the exhaust is six. These results hold for both the warmed up and the cold idle conditions, with the exception of E85 at cold idle because of the difficulty in fuel evaporation. The dependence of the organic gas emissions on injection timing may be divided into three regimes. With early injection, the fuel bounce from the piston results in high emissions. With injection in mid stroke, the emissions are low and not sensitive to the fuel pressure. With injection close to the bottom of the stroke, the interaction of the fuel deposit on the wall and the piston (which comes up shortly) results in higher emissions. The behavior is similar for all the ethanol/gasoline blends with the exception of E85 under cold idle condition.

1. INTRODUCTION

The direct injection spark ignition (DISI) engine could offer substantial benefit in specific power and fuel economy. Early introduction [1, 2] uses a lean stratified concept which leads to significant increase in part load fuel conversion efficiency mainly because of the reduction in throttle loss and better specific heat ratio of the working fluid. To meet the increasingly stringent emissions regulation, however, stoichiometric operation is required so that the 3-way catalyst could be utilized [3, 4]. Under stoichiometric operation, DISI still offers substantial advantage because of the charge cooling effect created by the in-flight fuel droplet evaporation. The cooling leads to better volumetric efficiency and knock margin. The latter is an enabler for realizing the turbo-charge/downsizing concept [5-7], which significantly reduces fuel consumption: by operating at a higher load point under cruise condition to reduce the relative friction losses, and by regaining the load head-room via turbo-charging.

The DISI engine hydrocarbon (HC) emissions have been a challenge [3, 9-11]. The cold start emissions, which contribute predominantly to the total trip emissions since the catalyst has not reached light-off temperature, are especially problematic. The difficulty is caused by:

- (i) The high pressure fuel pump could not maintain the required fuel pressure in the cranking process [9, 11]; then atomization and fuel evaporation are poor.
- (ii) The gas temperature is not high enough for significant droplet evaporation so that a substantial amount of liquid fuel lands on the cylinder walls [9, 10]. It is noted that although the metered fuel required for a stable start-up process is less for a DISI than for a port-fuel-injection (PFI) engine, the amount of fuel retained in the cylinder and the engine out HC emissions are significantly higher, even when an independently pressurized fuel injection system is used [9].

Practical solutions to the cold start HC problem have been developed. In the cranking process, fuel is injected during compression so that the higher ambient pressure assists atomization; optimization between the instantaneous fuel pressure and the amount of enrichment is sought [11]. In the warm up process, the strategy is to obtain an overall system (engine plus catalyst) optimization by using split injection [3, 5, and 11]. In this strategy, the spark timing is significantly retarded (after TDC of compression) to produce a hotter exhaust (compared to normal timing), and, because of the lower fuel conversion efficiency, a higher mass flow rate through the engine for the same torque output. Both attributes contribute to a higher enthalpy flow to the catalyst and facilitate light-off. To maintain engine stability under the retarded timing, fuel is injected in two pulses, one in the intake phase and one in the compression phase; the fuel introduced in the latter creates charge stratification. Then, although the overall mixture is stoichiometric, the local mixture at the spark plug is rich: air/fuel (A/F) ratio of 10:1 has been observed using LIF measurement [3]. The stratification enables a faster burn and reduces cycle-to-cycle torque fluctuations.

With the renewable fuel mandate required in US and the world, ethanol has been increasingly introduced as a supplement to the petroleum based gasoline. Although most of the ethanol has been supplied as a low concentration blend to gasoline (E10), usages at high concentrations (E85 or E100) are also in practice in US and Brazil. There are two significant attributes of ethanol: first, the heat of vaporization is significantly higher (factor of 2.8) than that of gasoline; second, compared to gasoline, significantly more ethanol is required for forming a stoichiometric mixture. Thus there could be substantial evaporative cooling of the fuel air mixture due to the ethanol evaporation. The positive effect (relative to using neat gasoline) of these attributes is the charge temperature is lower so that the knock threshold and the volumetric

efficiencies could be improved. The chemistry of the ethanol also suppresses knock. The negative effect of these attributes is a much more problematic cold start [12-14], since fuel evaporation is more difficult.

The work described in this paper is motivated by the increasingly stringent HC emissions requirement for spark ignition engines, and the emerging use of ethanol/gasoline (gasohol) blends which renders the HC emissions much more problematic. Both aspects are important considerations for DISI engine operation. In the first part of the paper, the speciated engine-out organic gas (HC plus oxygenates) emissions from a DISI engine are reported, both under fully warmed up condition and under cold fast-idle condition. Then the un-speciated engine-out HC emissions are reported as a function of the engine operating parameters.

2. EXPERIMENT

The work reported here looks at the impact on engine-out organic gas emission due to the presence of ethanol in the fuel under stoichiometric operation. To focus on this aspect, only a single-injection strategy has been used in this study, since a split injection strategy would need the integrated considerations of catalyst light-off characteristics, engine stability, and secondary air injection strategy. These considerations are beyond the scope of this work.

2.1 Engine set up

The engine is the GM naturally aspirated DISI Ecotec 4-cylinder engine [15] which is modified for single cylinder operation. Cylinder no. 1 is the only active cylinder with the intake and exhaust separated from the remaining three cylinders, which are under wide-open-throttle (WOT) motoring operation. The engine is equipped with a charge motion control valve at the intake port to provide a swirling charge motion; see Fig. 1. The valve is closed (swirl-enabled) for all the experiments in this study. The engine specification is shown in Table 1.

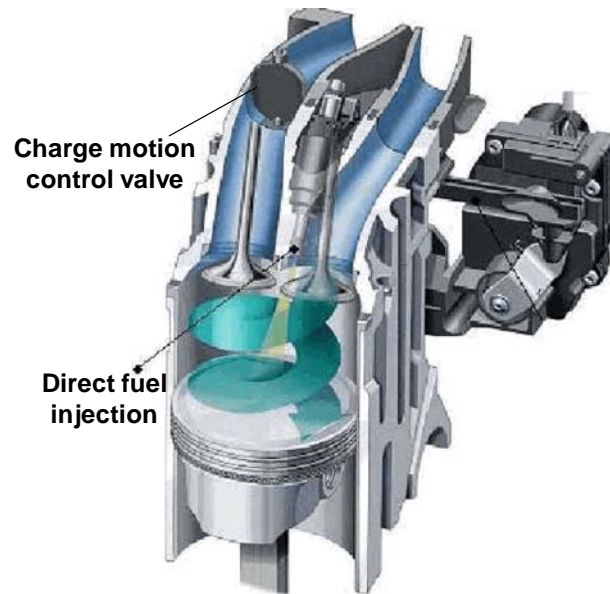


Fig. 1 Charge motion and injector arrangement; adapted from [15]

Table 1 Engine specification

Displacement per cylinder	550 cc
Bore	86 mm
Stroke	94.6 mm
Compression ratio	12.0
IVO/IVC	0° after TDC/60° after BDC
EVO/EVC	44.5° before BDC/10.5° after TDC
Injector Center Line	47° from horizontal
Nominal cone angle	52°
Injection pressure	40 to 120 bar

The engine coolant temperature (ECT) is controlled by a commercial chiller and heater combination. For experiments at ECT lower than ambient, the coolant is also used to control the fuel temperature through a heat exchanger; otherwise the fuel is not cooled. To control the injection pressure, the engine fuel pump is not used. Instead, premixed ethanol/gasoline blends were supplied from individual accumulators pressurized by high pressure nitrogen at 40 to 120 bar. (Depending on the load, the production engine calibration uses different injection pressure; a lower/higher pressure at low/high loads. The injection pressure is varied independently in this

study.) The fuel line is arranged that the residual fuel could be flushed out by running the engine for a short time. The flushing process is validated by observing the change in fuel pulse width under stoichiometric condition when the fuel is switched from gasoline to E85.

The fuel spray has a nominal cone angle of 52° , with the center line at 47° from the horizontal. The nominal spray is shown in Fig. 2, showing the relative spray cone geometry with respect to the flat piston at various crank angles from TDC. Note that the actual spray geometry will depend on the injection and cylinder pressure.

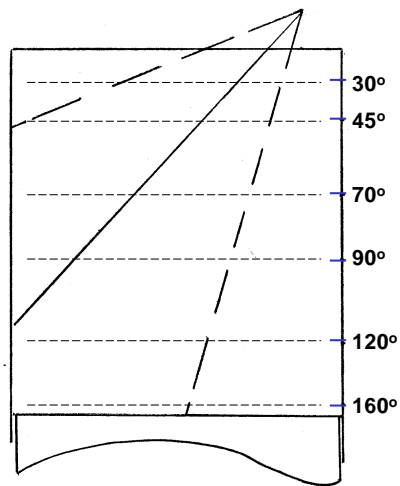


Fig. 2 Nominal spray geometry. The horizontal dotted lines mark the piston positions at the labeled values of crank angle after TDC

2.2 Gas sampling

The exhaust gas is measured by a Fast-Response-Flame Ionization Detector (FID) [16], and by a sampling system which holds the sample for Gas Chromatograph (GC) analysis. For the FID measurement, the sample inlet is located at 15 cm from the exhaust valve. The engine exhaust for the GC analysis is sampled from a mixing tank 2 m from the exhaust valve.

The sampling system [17, 18] for the GC analysis consists of 16 pre-evacuated sampling cylinders connected via individual 3-way solenoid valves to the sampling line; see Fig. 3.

Referring to the figure, the exhaust gas flows continuously through the by-pass line until the solenoid valve is activated for sampling. The sampling duration has been adjusted so that the final pressure of the sample is 15-17 kPa. Immediately after sampling, the sample is diluted with research-grade nitrogen (purity 1 part in 10^6) to 300 kPa. The pressures are measured by a pressure transducer (MKS Baratron 629B) to determine the precise dilution ratio. To prevent condensation of water vapor and heavy hydrocarbons, the whole system is kept at 150°C . With 16 sampling cylinders, exhaust gas samples under different engine conditions could be collected before the rather lengthy GC analysis. Most samples are analyzed within one day.

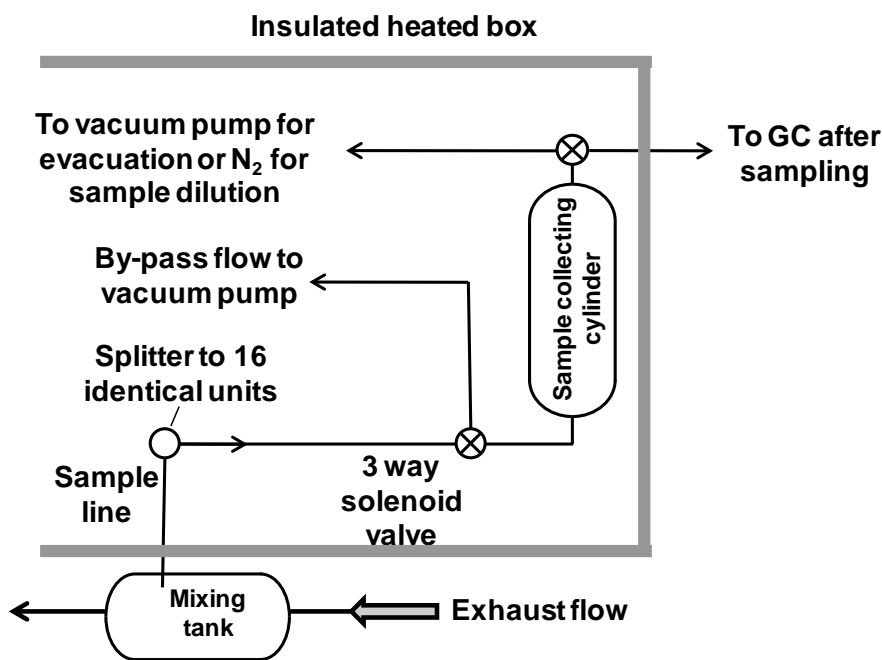


Fig. 3 Schematic of gas sampling system for GC analysis.

2.3 Gas chromatograph technique

The GC method is adapted from the one developed in the Auto/Oil Air Quality Research Program (AQIRP) [19, 20] for engine exhaust organic gas speciation. The procedure has been well established and a GC library containing the retention time of 150 species is available. Only a brief description of the analytical method is given here; see references [19, 20] for more details.

Exhaust GC analysis is performed on a Hewlett Packard Model 5890C Series II GC. Exhaust gas samples are introduced into a six-port rotary switching valve. This valve allows a fixed volume of gas sample to be maintained at a known pressure and temperature, and controls the injection of samples into the GC with millisecond resolution so that retention times are highly repeatable. Each sample is then directed through a split injector. Only 1/5 of every sample enters the column; the remainder is vented. The gas mixture is separated in a 60-meter column in 54 minutes and species are detected by a FID. Unlike the original method in [18], a make-up gas of helium is used instead of nitrogen. This use only changes the sensitivity of the detector (counts/ppmC1), which has been accounted for in calibration. Table 2 lists the GC parameters used in this study.

Table 2. Summary of GC analysis parameters

Instrument	HP5890 Series II Gas Chromatograph
Column	60 m DB-1 (Agilent) 0.32 mm ID, 1 μ m film thickness
Sample Loop	2.0 mL
Sample Loop and valve temperature	120°C
Split ratio	5.2:1 (injection volume = 0.38 mL)
Injector temperature	200°C
Carrier gas	Helium >99.999%, 145 kPa to get 7.0 mL/min at -80°C
Detector Type	FID
Detector temperature	300°C
Detector hydrogen	>99.999%, 110 kPa
Detector air	<0.1% total hydrocarbon, 285 kPa
Detector make-up gas	Helium, >99.999%, 275 kPa to achieve 32 mL/min
Separation programming	-80°C for 0.01 min -80°C to -50°C at 20°C/min -50°C for 2.5 min -50°C to 250°C at 6°C/min

The species are identified by their retention times. The calibration is done via a 23 component gas reference (CRC Mixture #4, developed for the AQIRP) consisting of normal alkanes from C1-C12, and other representative compounds. See Table 3 for composition. The species are identified by a retention index (RI), which is computed from the individual retention time relative to that of the reference normal alkanes in the calibration gas:

$$RI = 100n + 100 \frac{t_x - t_n}{t_{n+1} - t_n} \quad (1)$$

where

t_x = retention time of unknown species x

t_n = retention time of n-alkane eluting prior to x

t_{n+1} = retention time of n-alkane eluting immediately after x

n = carbon number of n-alkane with retention time t_n

Table 3. Calibration mixture for GC analysis

Peak number	Compound	Concentration (ppmC1 \pm 95% confidence interval)	Retention index
1	Methane	4.98 \pm 1.8%	100.0
2	Ethylene	3.03 \pm 2.7%	158.1
3	Ethyne	1.10 \pm 1.7%	187.3
4	Ethane	4.96 \pm 1.2%	200.0
5	Propane	9.16 \pm 1.4%	300.0
6	2-methylpropene	4.99 \pm 2.9%	390.5
7	1,3-butadiene	5.21 \pm 3.1%	395.1
8	n-butane	5.18 \pm 3.1%	400.0
9	n-pentane	5.01 \pm 1.9%	500.0
10	n-hexane	4.72 \pm 2.5%	600.0
11	Benzene	4.66 \pm 2.3%	649.7
12	2,2,4-trimethylpentane	4.93 \pm 2.6%	689.9
13	n-heptane	4.92 \pm 2.5%	700.0
14	Toulene	5.08 \pm 3.0%	756.8
15	n-octane	5.01 \pm 2.9%	800.0
16	p-xylene	5.13 \pm 5.0%	862.7
17	o-xylene	5.15 \pm 5.1%	865.1
18	n-nonane	5.01 \pm 2.9%	900.0
19	1,2,4-trimethylbenzene	3.16 \pm 3.7%	989.0

20	n-decane	$5.36 \pm 3.1\%$	1000.0
21	n-undecane	$4.98 \pm 4.2\%$	1100.0
22	n-dodecane	$3.75 \pm 3.3\%$	1200.0
23	n-tridecane	3.0	1300.0

The species are identified by matching the calculated RI to the ones in the GC library. For the identified species, the HP ChemStation software (version A. 10.02) is used to obtain the area count under the individual peak of the chromatogram. The software has provision to resolve overlapping peaks. A species specific response constant k_i is used to relate the area count to the concentration of species i (in ppmC1). For the 23 species listed in Table 3, the values of k_i are obtained from the chromatogram of the calibration gas of known concentrations [18]. For other HC species, the response constant of propane is used. For ethanol and acetaldehyde, using the measurements in Ref. [21], $k_{\text{ethanol}}/k_{\text{propane}} = 0.74$ and $k_{\text{acetaldehyde}}/k_{\text{propane}} = 0.67$. Formaldehyde cannot be detected since the FID does not respond to it.

With the procedure described in the above, 80-90% of peaks in the chromatograph could be identified. The cumulative area under the identified peaks is 95% of the total area.

2.4 Fuels and test conditions

The fuel is a mixture of certification gasoline (Chevron Philips UTG91) and anhydrous ethanol (Pharmco-Aaper 200 proof, 99.98% purity). . The mixture is designated by a E number; e.g. E0 corresponds to neat gasoline, and E85 correspond to a blend with 85% by liquid volume of ethanol. The fuel ranges from E0 to E85. The distillation curve of the gasoline and the normal boiling points of ethanol and several fuel hydrocarbons are shown in Fig. 3. That the ethanol normal boiling point is substantially lower than that of most of the fuel components implies that ethanol would be preferentially distilled in the evaporation process of the fuel blend. The high latent heat of vaporization of ethanol will cool the fuel and renders evaporation of the remaining fuel more difficult

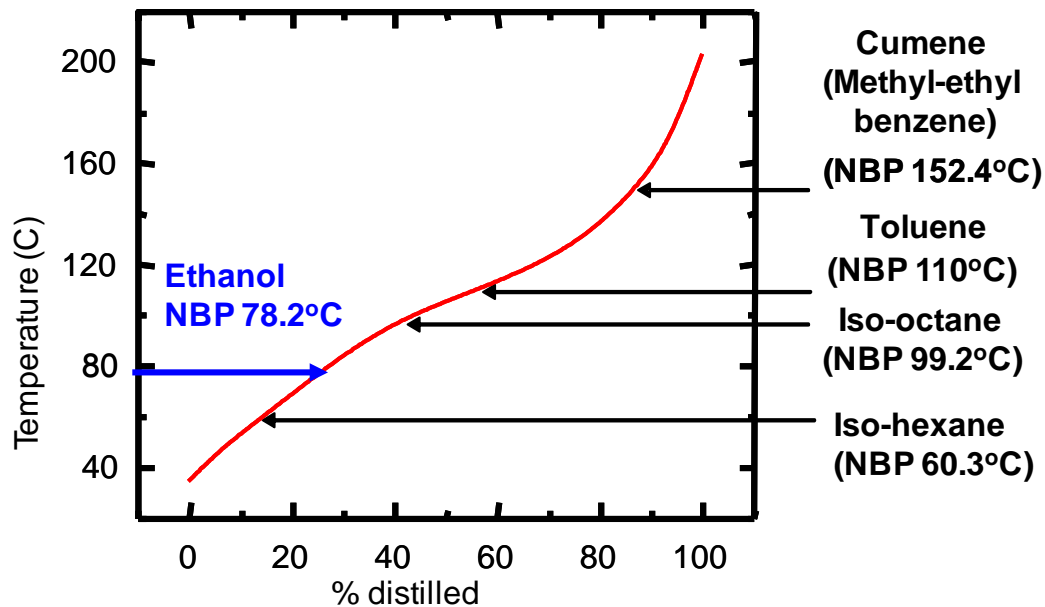


Fig. 4 Distillation curve (ASTM D86) for certification gasoline UTG91 and the normal boiling points of ethanol and several fuel hydrocarbons. UTG91 has a RVP of 64.4 kPa.

For the tests at fully warm up condition (ECT = 80° C), the operating point is at 1500 rpm, 3.8 bar net indicated mean effective pressure (NIMEP) with Maximum-Brake-Torque (MBT) spark timing. For the cold fast idle condition, the ECT is 20° C; the operation point is at 1200 rpm and 0.27 bar MAP. The NIMEP is 1.5 bar. The spark timing is 15-17° before TDC, which is 5° retarded from MBT timing. The air equivalence ratio (λ) is kept at 1 with a feedback controller using an UEGO sensor. The injection timing for the specific tests are described in the results section.

3. RESULTS AND DISCUSSION

3.1 Speciated Organic gas emissions under warmed up and under cold fast idle conditions

The speciated HC emissions have been obtained at the fully warmed up and under cold fast idle conditions as described in the last section. The injection pressure is 70 bar. The end of injection is at 120° after TDC of intake. The results are in terms of the mole fractions of the various species, and in terms of a mass based emission index so that a fuel-to-exhaust “feed-through”

rate could be obtained for the different species. To connect with conventional measurement, the total organic gas emissions are also expressed in terms of carbon mole fraction (ppmC1).

3.1.1 Speciated Emissions

The overall organic gas emissions (i.e. including ethanol and acetaldehyde emissions) in terms of ppmC1 are shown in Fig. 5 for the two test conditions. For the warmed up engine, the emissions decrease with the increase of ethanol content in the fuel. For the cold engine, the emission level is significantly higher (approximately a factor of 2.5 for ethanol content $\leq 50\%$); the dependence on the ethanol content, however, has the same slope as that of the warmed up engine except for the E85 fuel. For the E85 fuel at $ECT = 20^\circ C$, because of the high concentration of ethanol, there is substantial cooling due to vaporization. As a result substantial amount of fuel that is deposited on the wall may be end up in the piston crevice and contribute to exhaust emission. This subject will be discussed again in Section 3.3.2.

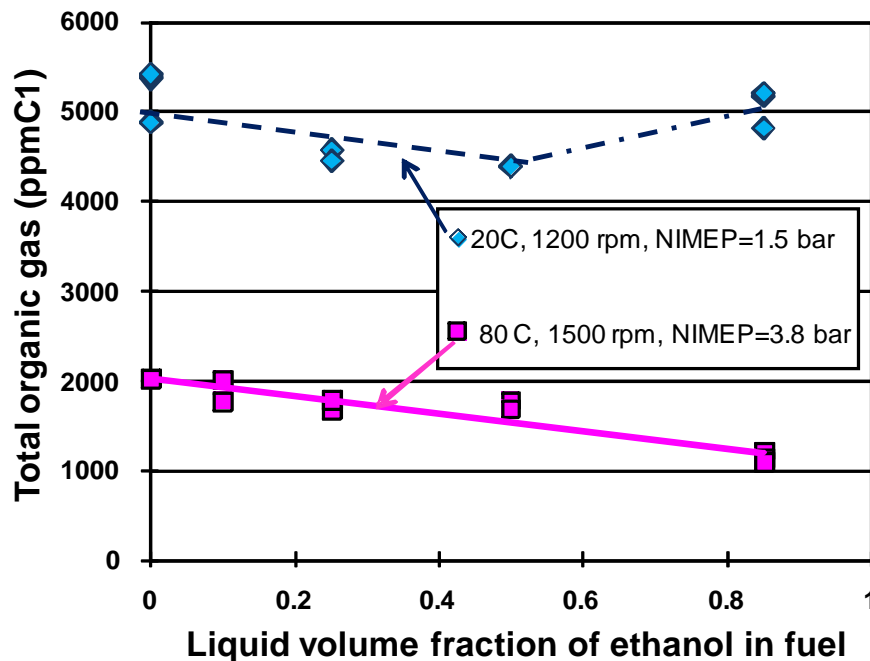


Fig. 5 Engine out total organic gas emissions (in ppmC1) as a function of liquid volume fraction of ethanol in the ethanol/gasoline blend.

The mole fraction of ethanol in the exhaust organic gas as a function of the volume fraction of ethanol in the fuel blend is shown in Fig. 6 for the two test conditions. There is a small systematic error due to the ethanol emission from the lubrication oil, since no ethanol emission is expected for E0. Operationally, to change lubrication oil for every run and wait for the oil to come to equilibrium with the run condition would take a long time. Since the systematic error is not large and we are interested in the incremental change in emission with fuel blends, the error is deemed acceptable. The ethanol emission increases linearly with the fuel ethanol content for the warmed up engine; the slope is 5.5 percentage points per every 10 percentage points increase in ethanol volume fraction in the fuel. Except for E85, which is the outlier as previously discussed, the ethanol mole fraction in the exhaust organic gas for the cold engine is almost identical to that of the warmed up engine if the offset due to the emission from the lubrication oil is subtracted.

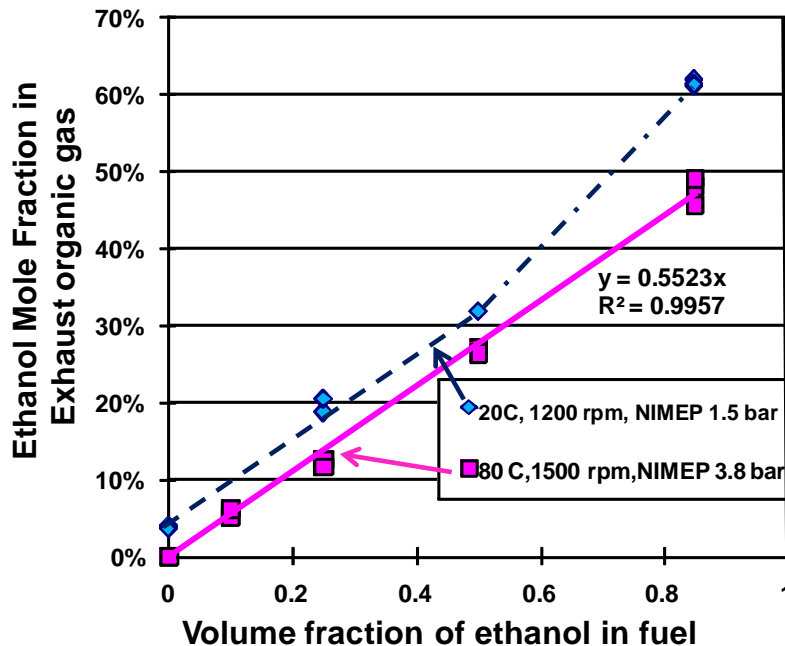


Fig. 6 Engine out ethanol mole fraction in the exhaust organic gas as a function of liquid volume fraction of ethanol in the ethanol/gasoline blend.

The distributions of the species in the exhaust for the two operating conditions are shown in Fig. 7 and 8. In these figures, only the major species (i.e., with mole fraction larger than or equal to 3% in the exhaust of at least one of the fuel blends) are shown. The remaining species are grouped together and labeled as “others”. As the ethanol content in the fuel increases, the oxygenates (ethanol and acetaldehyde) increase correspondingly in the exhaust.

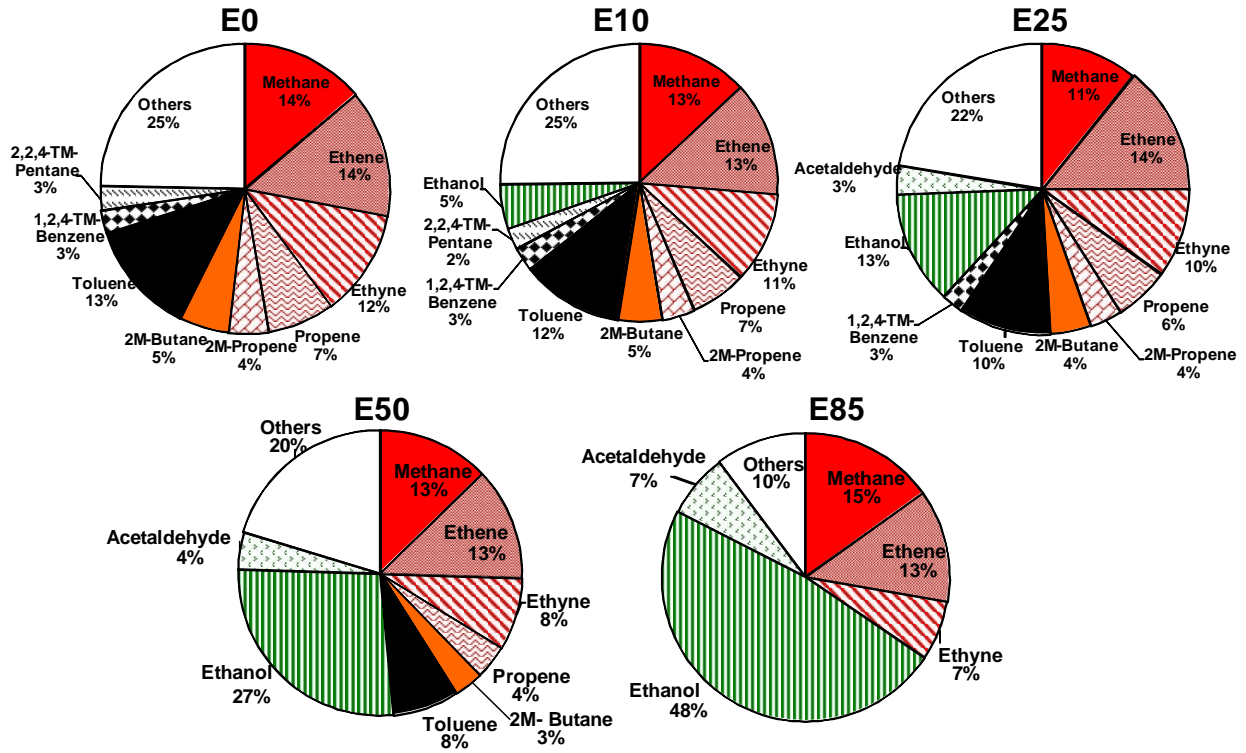


Fig. 7 Distribution of species (as mole fraction) in the exhaust of ethanol/gasoline blend at the warmed up condition (1500 rpm; $\lambda = 1$; 3.8 bar NIMEP; $\text{ECT} = 80^\circ \text{C}$).

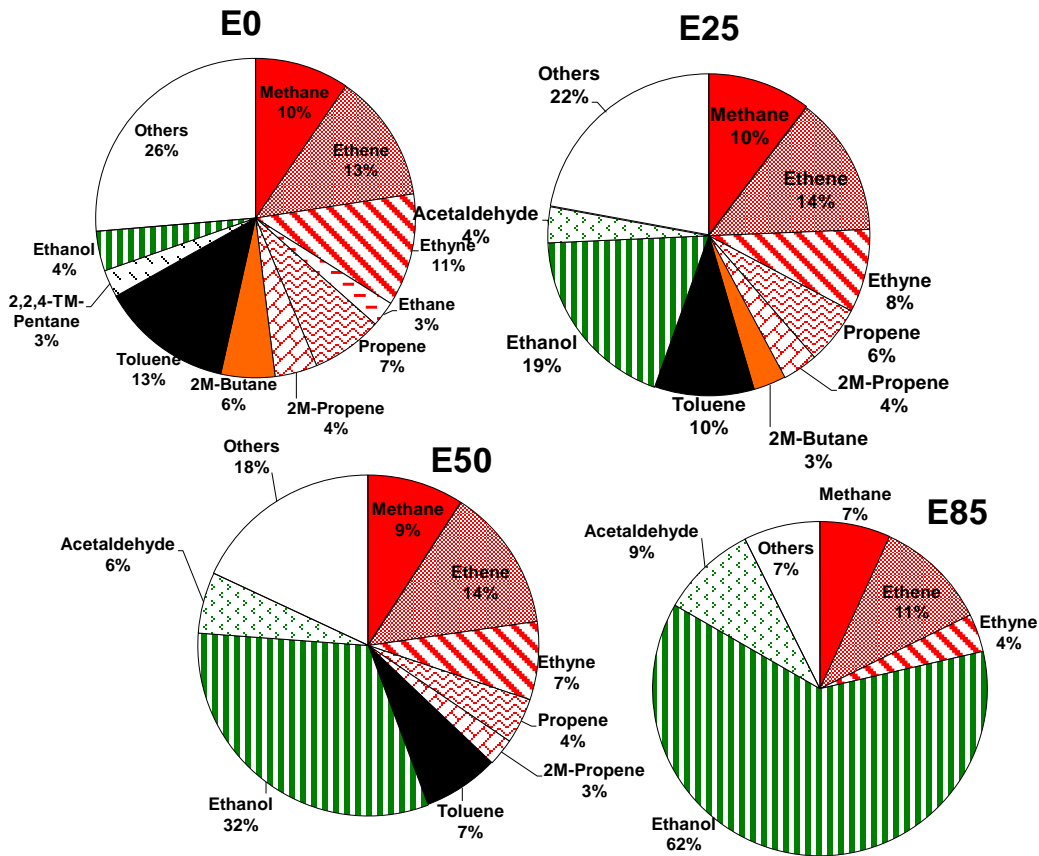


Fig. 8 Distribution of species (as mole fraction) in the exhaust of ethanol/gasoline blend at the cold fast idle condition (1200 rpm; $\lambda = 1$; 1.5 bar NIMEP; $\text{ECT} = 20^\circ \text{C}$).

It is noted that there is significant presence in the exhaust of acetaldehyde, which is an intermediate species in the ethanol oxidation process, when the ethanol content of the fuel increases. The correlation between the two species in the exhaust is shown in Fig. 9. The ratio of the ethanol to acetaldehyde emission is approximately six (by mole) for both the cold and the warm conditions, and for the variations of ethanol contents in the fuel.

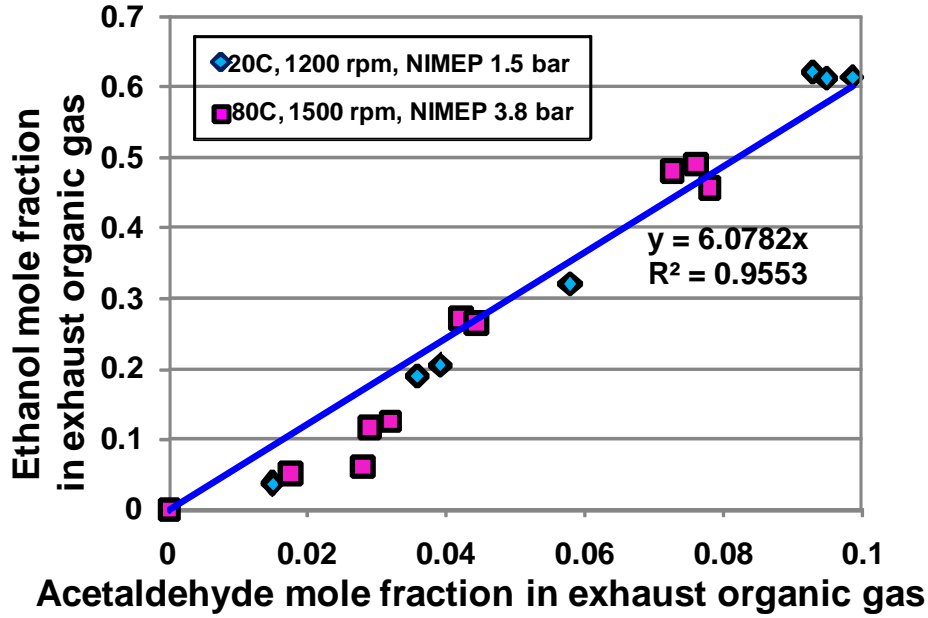


Fig. 9 Ethanol versus acetaldehyde mole fractions in the exhaust; for both warmed up and cold fast idle conditions.

3.1.2 Emissions index

It is of interest to express the speciated emissions data as species masses. A mass based Emission Index (EI) for species i is defined as:

$$EI_i = \frac{m_{e,i}}{m_f} \quad (2)$$

Here $m_{e,i}$ is the mass of species i in the exhaust per engine cycle, and m_f is the fuel mass per cycle. The value of $(EI)_i$ is calculated from the exhaust species mole fraction and molecular weight, the average molecular weight of the exhaust, and the air/fuel ratio. The mass fraction of the fuel species in the fuel ($m_{f,i}/m_f$) is known. (The particular batch of UTG91 gasoline used in the experiment has been sent to a commercial analytical firm to be analyzed.) Then in a plot of $(EI)_i$ versus $m_{f,i}/m_f$ for the fuel species that appears in the exhaust, the slope is:

$$\text{Slope} = \frac{m_{e,i}/m_f}{m_{f,i}/m_f} = \frac{m_{e,i}}{m_{f,i}} \quad (3)$$

This quantity can thus be interpreted as the individual fuel-to-exhaust “feed-through” rate [22].

The emission index for ethanol versus the ethanol mass fraction in the fuel is shown in Fig. 10. The variation of the fuel species in the fuel in this and the subsequent results has been obtained by the changing the ethanol content in the fuel. The feed-through rate for the warmed up engine is 0.52%; i.e. 0.52% (by mass) of the ethanol in the fuel appears as engine-out ethanol emission. The value for the cold engine is higher, at 1.88% (except for E85, which is an outlier as explained earlier.)

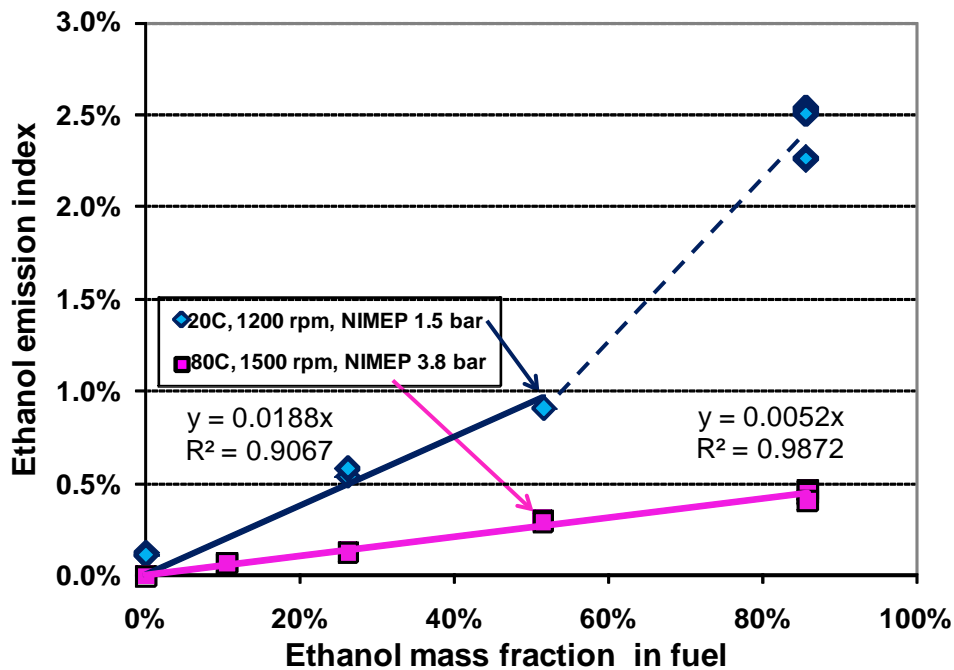


Fig. 10 Ethanol emission index versus its mass fraction in the fuel; for both warmed up and cold fast idle conditions.

The emission indices for the small fuel alkane species (up to C6) in the exhaust is shown in Fig. 10 and 11. The feed-through rate for the warmed up engine is somewhat higher than that of ethanol (0.65 versus 0.52%); that for the cold engine, however is lower (1.48 versus 1.88%).

The feed-through result from the Auto-Oil Program [22] is also shown in Fig. 11 for comparison.

It should be noted that the result from that program has been obtained from vehicle driving cycle data; the current results have been obtained from two specific engine operating points.

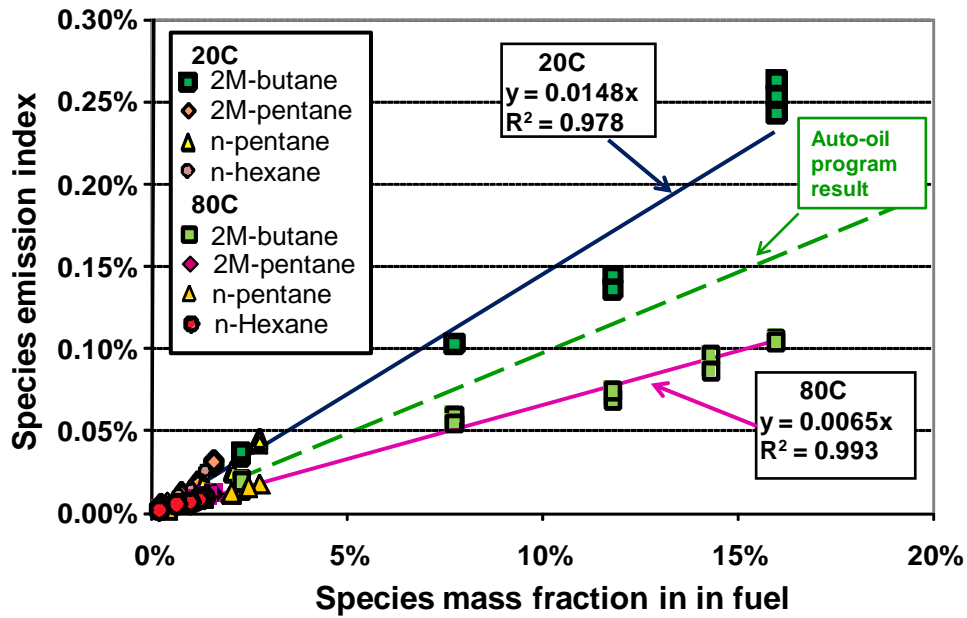


Fig. 11 Emission indices for paraffinic species versus their mass fraction in the fuel; for both warmed up and cold fast idle conditions.

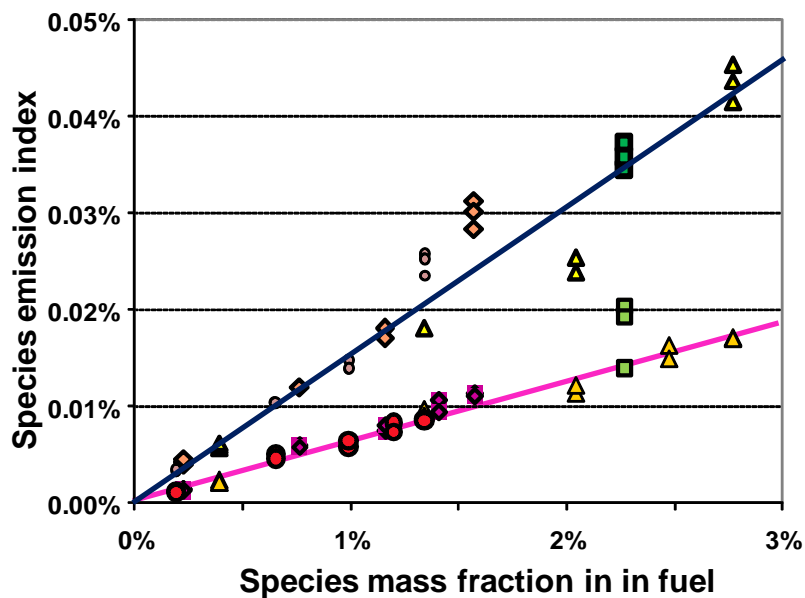


Fig. 12 Magnified view of Fig. 12 for data in the lower left corner. See Fig. 11 for legends.

The emission indices for the aromatic species are shown in Fig. 13 and 14. The feed-through rates for both the warmed up and cold engine conditions are higher than those of ethanol and alkanes. The value for the warmed up engine is approximately the same as that observed in the Auto-Oil Program [22].

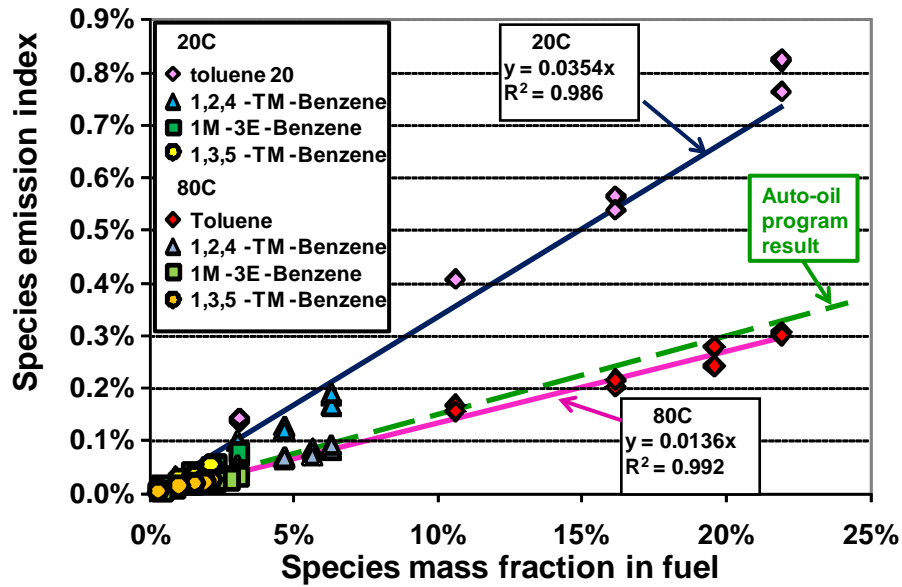


Fig. 13 Emission indices for aromatic species versus their mass fraction in the fuel; for both warmed up and cold fast idle conditions.

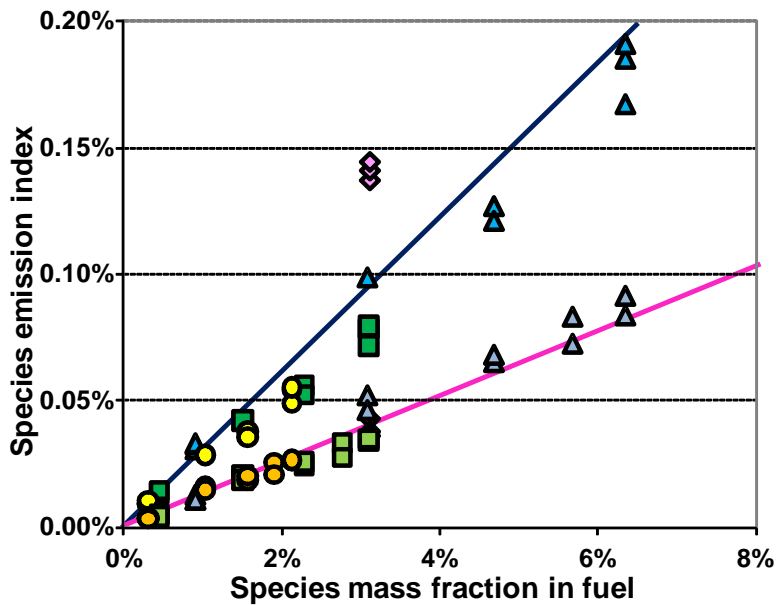


Fig. 14 Magnified view of Fig. 13 for data in the lower left corner. See Fig. 13 for legends.

3.2 HC emission as a function of engine operating parameters

To investigate the effect of fuel and engine parameters on HC emissions, data have been obtained at two test conditions. The first set of tests was done at intake pressure of 0.47 bar (NIMEP ~4.5 bar) so that a substantial amount of fuel was injected per cycle (17 mg for E0). Most of these tests were with gasoline to examine the effects of injection timing, ECT and pressure on HC emissions. The second set of tests was done at intake pressure of 0.27 bar (NIMEP ~ 1.5 bar) which represents the fast idle condition. Substantially less fuel was injected (10 mg for E0) compared with the first set of tests. The focus of this test set is on assessing the fuel effects. All tests were done at 1200 rpm and $\lambda = 1$. The spark timing was at 17° before TDC; the timing was 3 to 5° retarded from MBT timing.

Because of the substantial effort required for speciation analysis, the HC emissions for these parametric tests have been measured with a FID only. As discussed above, because the FID has a different response function to the exhaust oxygenates, the HC emissions cannot be compared directly from fuel-to-fuel. However, common features could still be discerned in the HC dependence on engine parameters such as injection timing and ECT.

3.2.1 HC emissions of gasoline at medium load

The general feature of the HC emissions as a function of end-of-injection (EOI) timing is shown in Fig. 15 for E0 at 1200 rpm, 4.5 bar NIMEP and $\lambda = 1$. The ECT was at 60° C and injection pressure was at 70 bar. (Effects of ECT and injection pressure will be shown later.) The injection (of 12.5 CAD duration; see Fig 15) was arranged such that it always occurred after the exhaust valve was closed so there was no short circuiting of fuel to the exhaust port. For comparison, the HC emissions from using isopentane as fuel are also shown. Because of its high

volatility (NBP at 27.7° C), isopentane flash-boils; so it may be considered as a gaseous fuel.

The relative piston position and piston speed are also shown as reference.

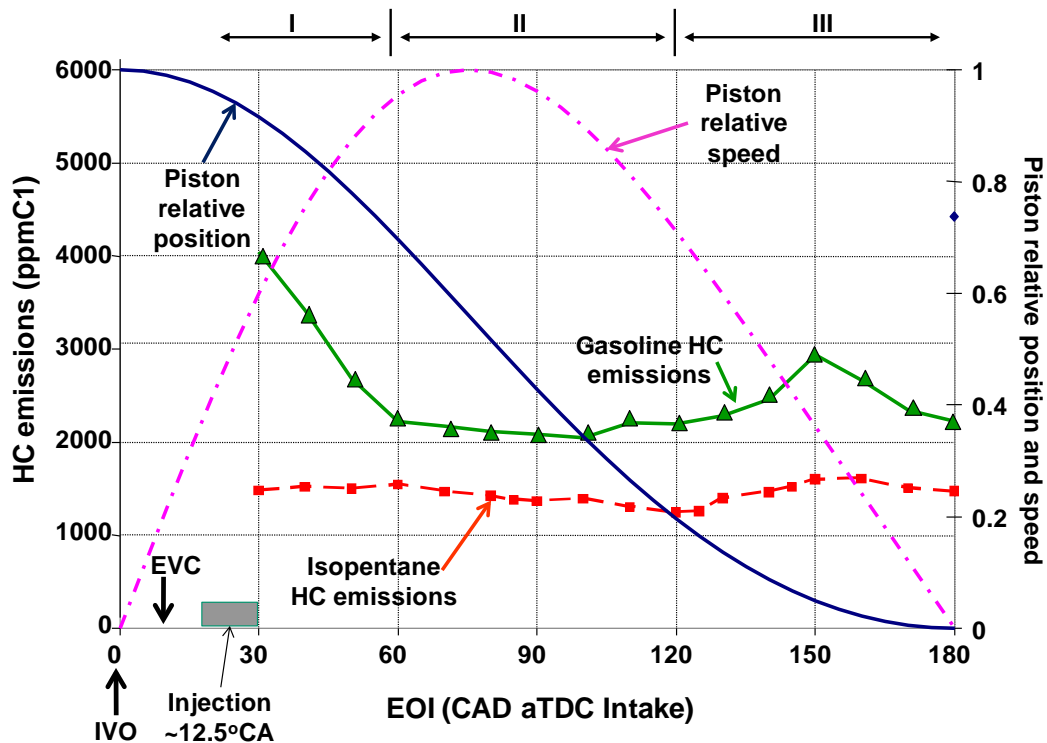


Fig. 15 Engine out HC emissions using gasoline and isopentane, as a function of end-of-injection (EOI) timing. The piston relative position and speed are also shown. Engine operated at 1200 rpm, 4.5 bar NIMEP, $\lambda = 1$, 17° BTDC spark timing, ECT = 60° C, and 70 bar injection pressure.

While for isopentane, the HC emissions behavior is almost flat with respect to EOI, for gasoline, three regimes of behavior are observed in Fig. 15. When injection is early (regime I), the HC emissions are high, but decrease rapidly and become flat with respect to EOI in regime II (mid-stroke). Then when EOI is at close to the bottom of the stroke (regime III), HC emissions increase again.

The gasoline HC emissions behavior for three different injection pressures is shown in Fig. 16. The behavior is similar to that for 70 bar injection pressure (Fig. 15). The three regimes of behavior are identifiable, with the HC emissions somewhat higher with higher injection

pressure in regime III. The emissions for EOI in regime II is not sensitive to injection pressure; see Fig. 17.

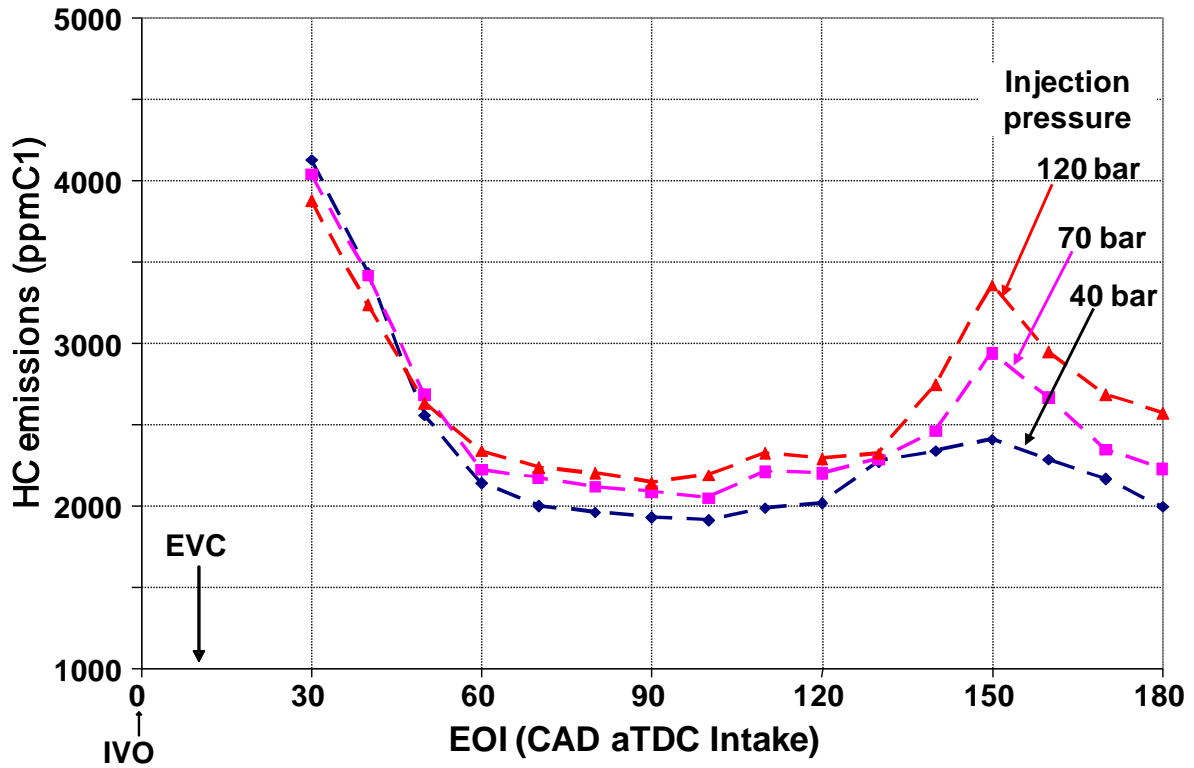


Fig. 16 HC emissions as a function of EOI. Operating condition is the same as that in Fig. 15 except for fuel pressure.

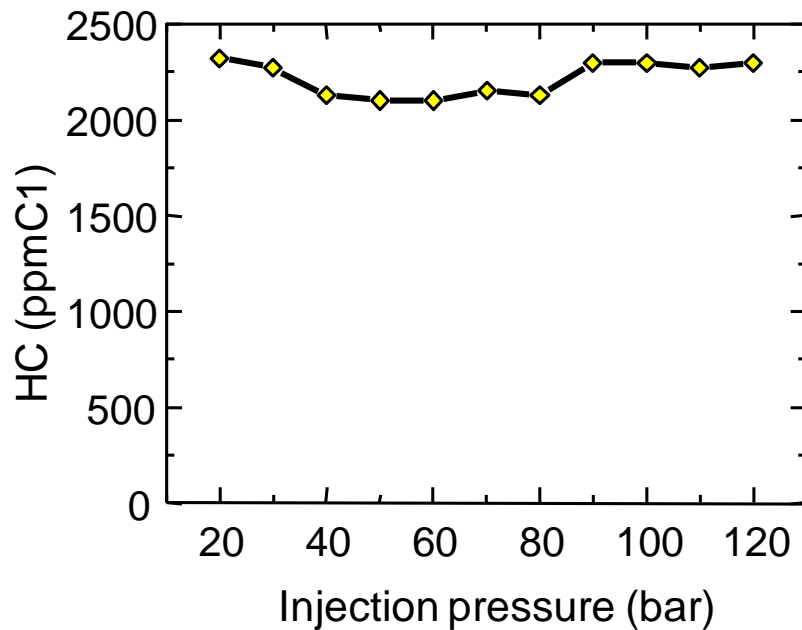


Fig. 17 HC emissions as a function of fuel pressure. Operating condition is the same as in Fig. 15, except for fuel pressure; EOI was at 120° CA after TDC intake.

The HC emissions dependence on EOI may be explained in reference to the piston position during the injection process. (Piston relative position is shown in Fig. 15 and combustion chamber and spray geometry at different piston positions is shown in Fig. 2.) When EOI is in regime I, because of the proximity of the injector to the piston, the fuel spray would substantially bounce off the piston and some of the liquid fuel lands on the head. The fuel that lands on the head, especially that lands at the vicinity of the exhaust valve, would contribute to “extra” HC emissions. (The fuel that lands on the piston does not contribute to “extra” HC emissions because its role is similar to the fuel that lands on the piston when EOI is in regime II.) As the piston descends, the fuel landing on the head decreases rapidly; hence the decrease in HC emissions observed in Fig. 15. Note that this phenomenon is not observed for the isopentane which is essentially a gaseous fuel.

When EOI is in regime II, the fuel droplets that land on the combustion chamber wall are spread over a large area, resulting in a very thin film that evaporates quickly. As an estimate of the film thickness, if all injected fuel (17 mg) is uniformly spread over an area of the piston (diameter 87 mm), the film would be 2.5 μm thick. Thus the film temperature would be the same as the wall temperature (since thermal equilibration time is in 10's of micro-seconds). Using normal alkanes as surrogates for fuel components with the same carbon number, the vapor pressure of the fuel species are shown in Fig. 18. The cumulative volume distribution as a function of carbon number is also shown in the figure. At ECT of 60° C and MAP of 0.5 bar, all components with carbon number up to C7 (i.e. slightly more than half of the fuel by volume) will flash-boil. The flash boiling facilitates the evaporation of the remaining fuel components. The evaporation and subsequent air/fuel mixing is further assisted by the charge motion because the fuel is injected in the region of maximum piston velocity. Therefore the HC emissions are not sensitive to the details of the injection when EOI is in regime II.

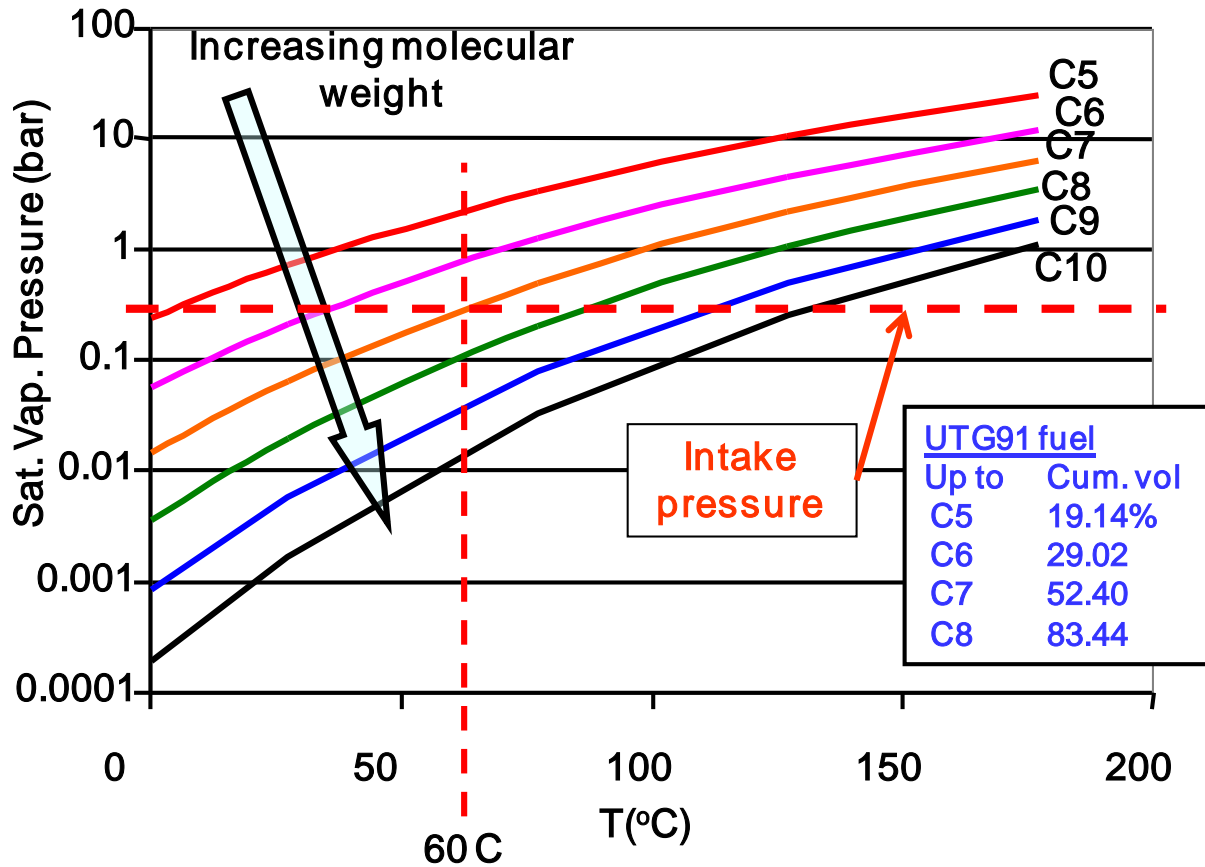


Fig. 18 Vapor pressure as a function of temperature for n-alkanes as surrogates for the gasoline fuel components with the same carbon number.

An explanation for the increase in HC emissions for EOI in regime III is as follows.

Here, some of the wall wetting liquid fuel lands on the cylinder wall area at the end of the stroke where locally the charge velocity is low so that air/fuel mixing is not as rapid. This fuel rich mixture pocket is immediately trapped in the crevice when the piston comes up, and contributes to the exhaust HC emissions through the crevice mechanism. (Note that the fuel vapor from the wall film formed with EOI in regime II has better mixing because of the higher piston velocity and more time to mix before being trapped in the crevice; hence the HC emissions is lower.)

The HC emissions, for EOI in regime II, as a function of ECT for gasoline and isopentane are shown in Fig. 19. For isopentane, which is essentially a gaseous fuel, the HC emissions are

primarily a crevice effect [23]. When ECT increases from 25 to 80° C, the trapped HC in the crevice decreases by about 12% because of the lower trapped gas density. The observed HC emissions, however, decreases much more (by 30%) because of the non-linear behavior of the crevice out-gas oxidation process [24]. The emissions from gasoline at the same ECT are higher, and the decrease in HC with increase in ECT is more rapid (more than a factor of 2). The gasoline HC emissions behavior may be interpreted as comprising a crevice mechanism and a liquid fuel mechanism. The former mechanism would yield a ECT dependence similar to that of isopentane; the latter, however, would significantly enhance the ECT dependence due to the sensitivity of fuel evaporation to temperature.

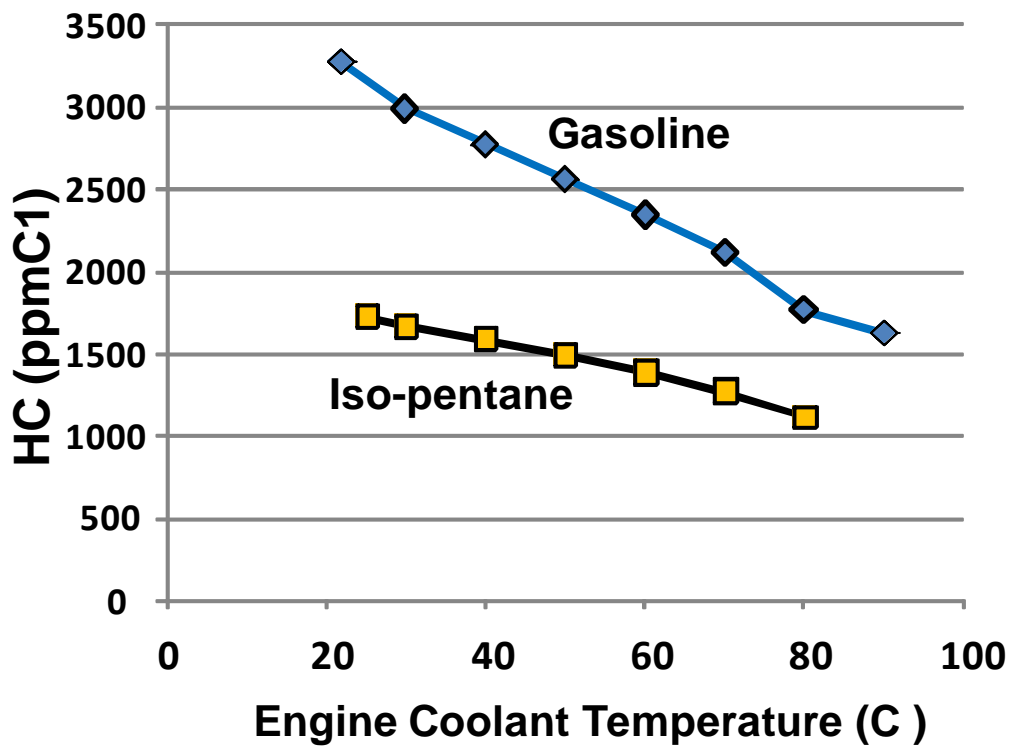


Fig. 19 HC emissions as a function of ECT. Operation condition is the same as in Fig. 15, except for ECT; EOI = 120° after TDC intake; injection pressure = 70 bar.

The HC emissions as measured by a FID for E85 as a function of injection timing is shown in Fig. 20. The operating condition is that same as that depicted in Fig. 15 for E0, but the

injection duration is longer due to the difference in stoichiometric requirement. The two results, however, could not be compared directly because the FID sensitivity to the exhaust gas is different for the two fuels. Nevertheless, the HC emissions as a function of EOI in Fig. 20 show the same feature as that in Fig. 15. Thus the discussion above for E0 also applies to E85.

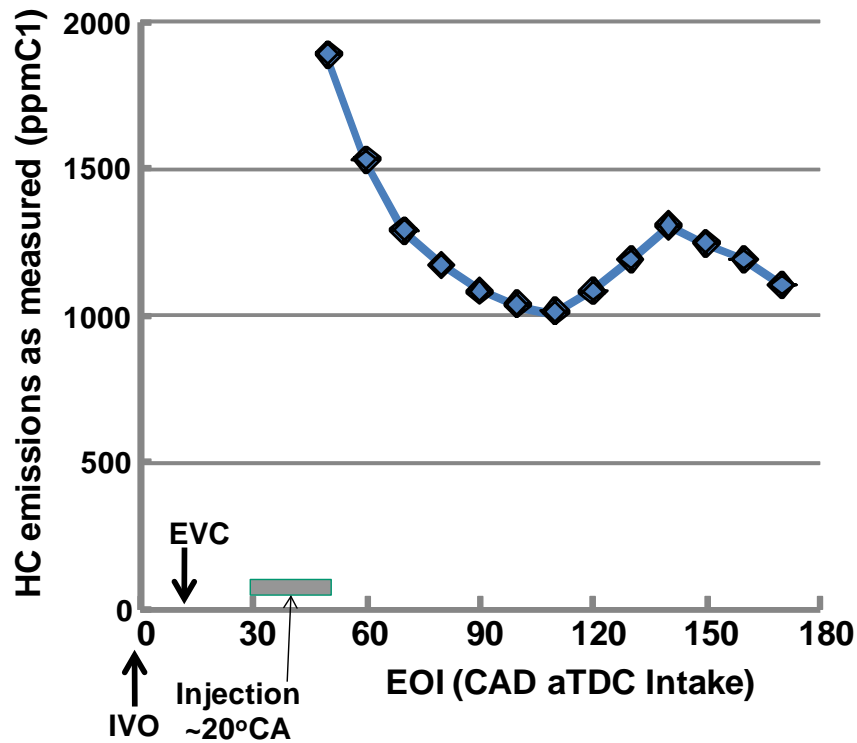


Fig. 20 HC emissions for E85 as a function of injection timing. Operating condition same as that of Fig. 14. The measurement is not corrected for the FID sensitivity to oxygenates.

3.2.2 HC emissions at fast idle

To assess the effects of fuel and engine operating parameters on engine-out emissions, the HC emissions in the exhaust have been measured with a FID as a function of EOI timing and ECT at 20°, 40° and 80° C for the following fuels: E0 (neat gasoline), E15, E40 and E85. The operating condition at 1200 rpm, 0.27 bar MAP (1.5 bar NIMEP) and $\lambda = 1$ is typical of the fast idle period. Spark timing has been set to 17° before TDC which is approximately 5° retarded from MBT timing. The fuel injection pressure has been kept constant at 70 bar. The FID signal

has been calibrated with propane and converted to a carbon mole fraction of ppmC1 without correcting for the lower FID sensitivity to oxygenates.

The HC emissions for E0 (gasoline) as a function of injection timing and ECT are shown in Fig. 21. Emissions decrease with increase in ECT. The emission dependence on EOI may be divided into three regimes in the same manner as in the higher load case (see Fig. 15), although at 80° C, the sharp drop of HC with increase of EOI timing in regime I (early injection) is not discernable.

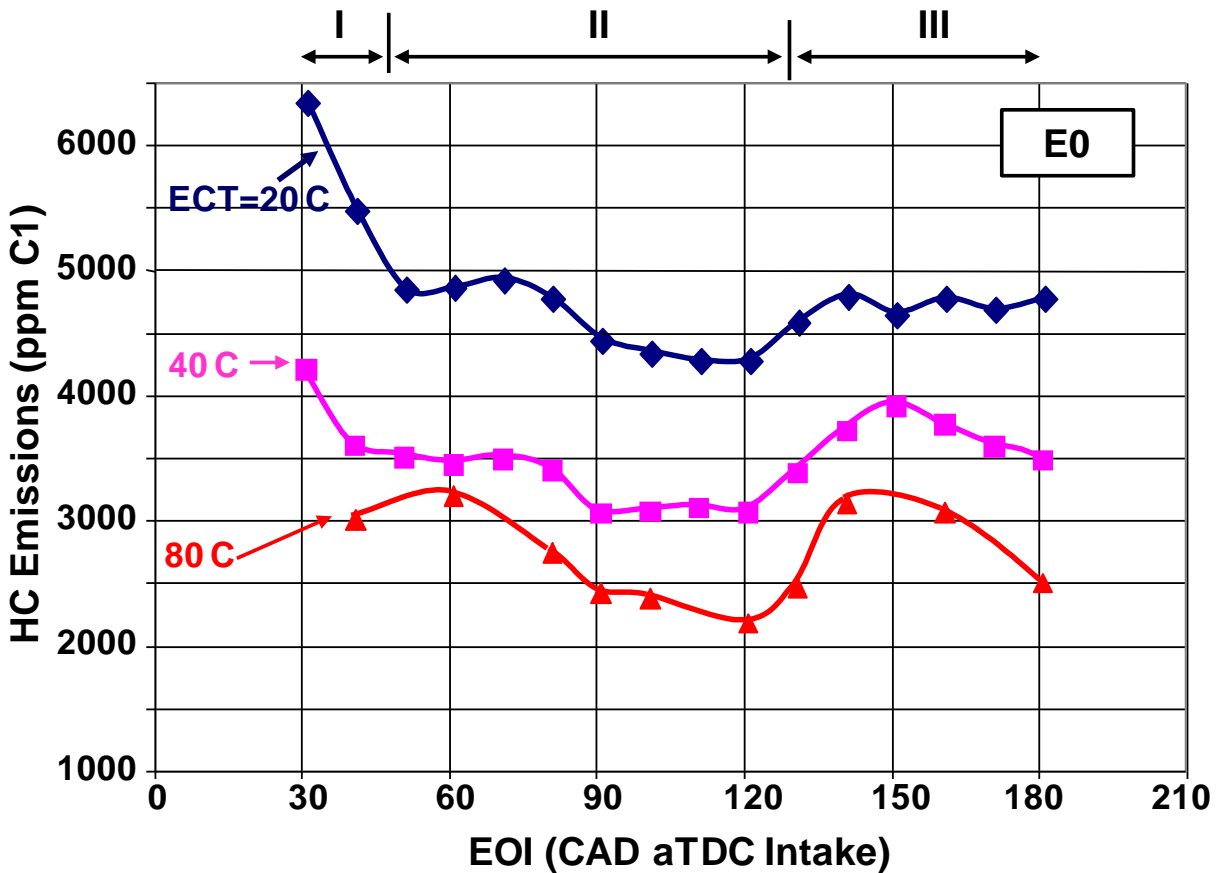


Fig. 21 HC emissions as a function of EOI timing and ECT for E0 (gasoline). Engine at 1200 rpm; $\lambda = 1$; MAP = 0.27 bar (NIMEP \approx 1.5 bar); injection pressure = 70 bar.

The apparent HC emissions (not corrected for the FID sensitivity to oxygenates) for E15 and E40 are shown in Fig. 22 and 23. The behaviors are similar to those of E0. The increase in

HC emissions in regime III (late injection) is less with E40. This observation may be explained by the significant presence of oxygenate in the fuel so that the trapped mixture in the crevice is less rich; thereby there is better post-combustion oxidation of the crevice gas.

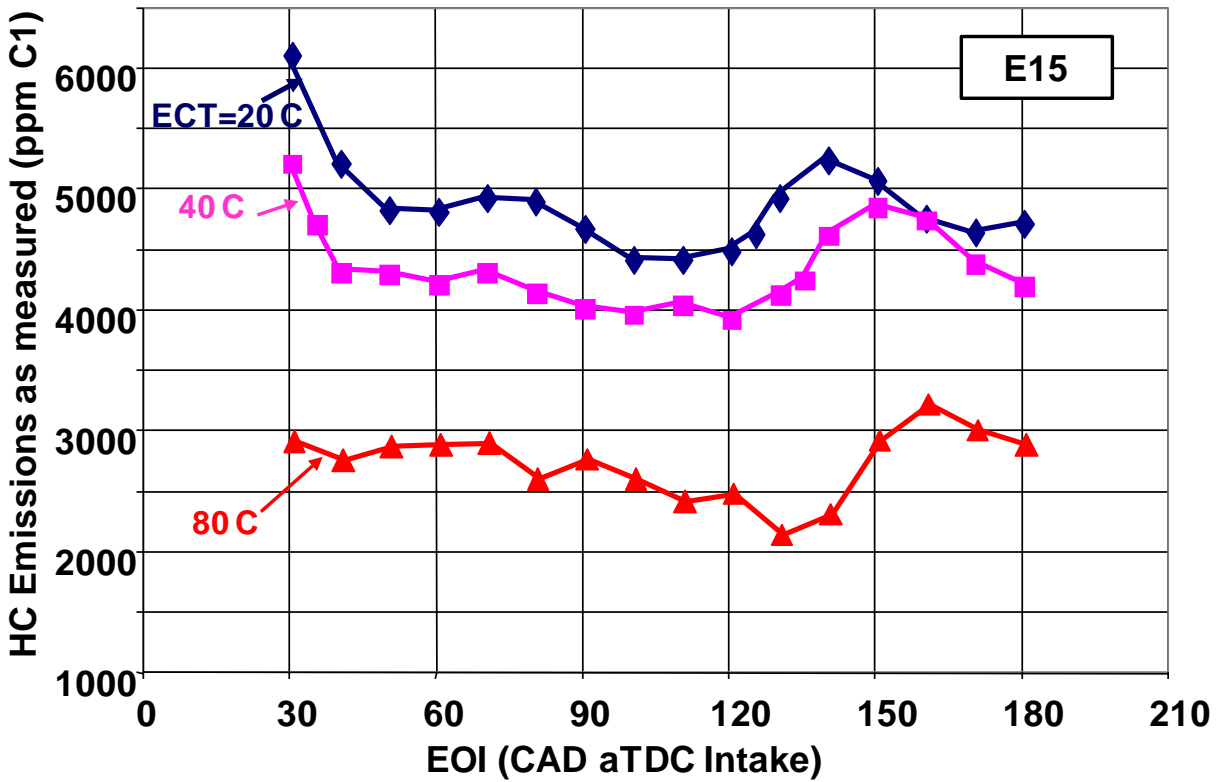


Fig. 22 HC emissions as a function of EOI timing and ECT for E15. Engine at 1200 rpm; $\lambda = 1$; MAP = 0.27 bar (NIMEP \approx 1.5 bar); injection pressure = 70 bar.

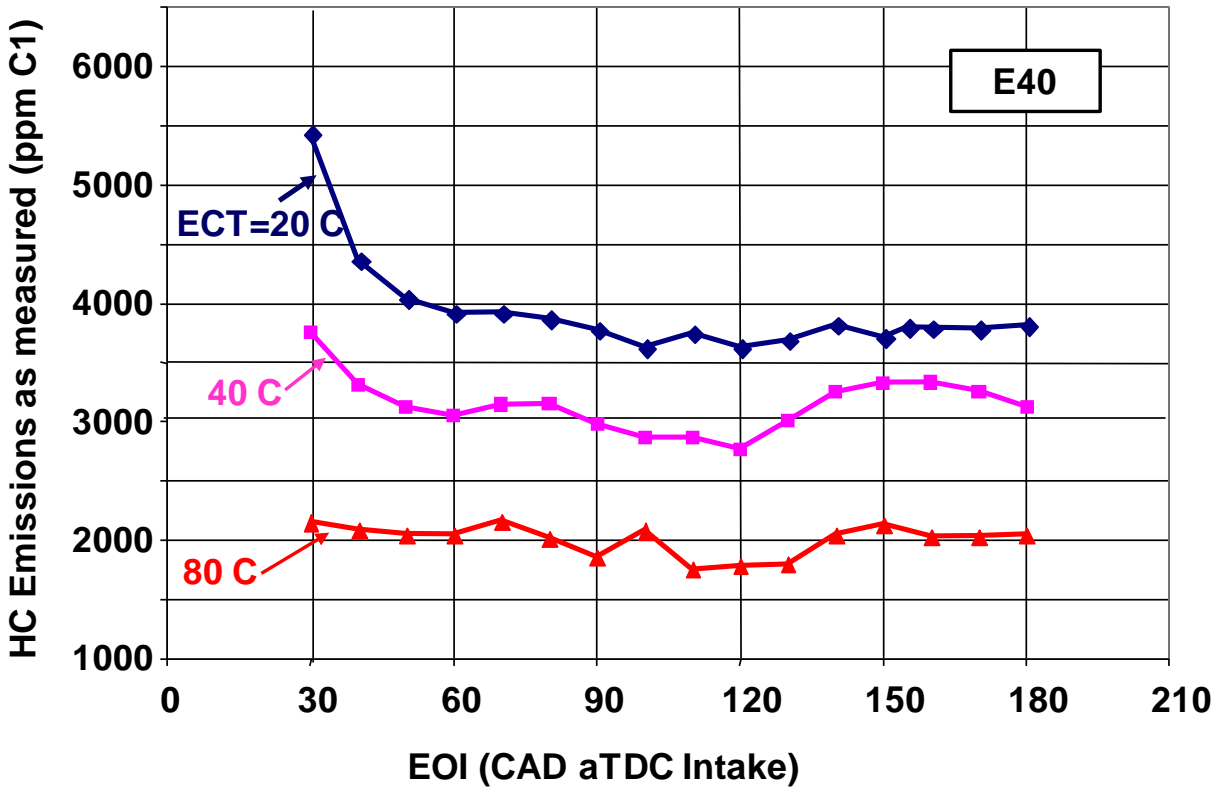


Fig. 23 HC emissions as a function of EOI timing and ECT for E40. Engine at 1200 rpm; $\lambda = 1$; MAP = 0.27 bar (NIMEP \approx 1.5 bar); injection pressure = 70 bar.

The HC emissions for E85 are shown in Fig. 24. The general behavior is similar to the E40 case (Fig. 23) except for the data at ECT = 20° C. Then there is a large increase in HC emissions with late injection. This observation may be explained by the portion of fuel delivered by the late injection to the bottom part of the combustion chamber, where the surface temperature is the lowest. Then the substantial latent heat of vaporization of the E85 fuel could result in sufficient local cooling to suppress evaporation. Trapping liquid fuel in the crevice would enhance the crevice HC mechanism.

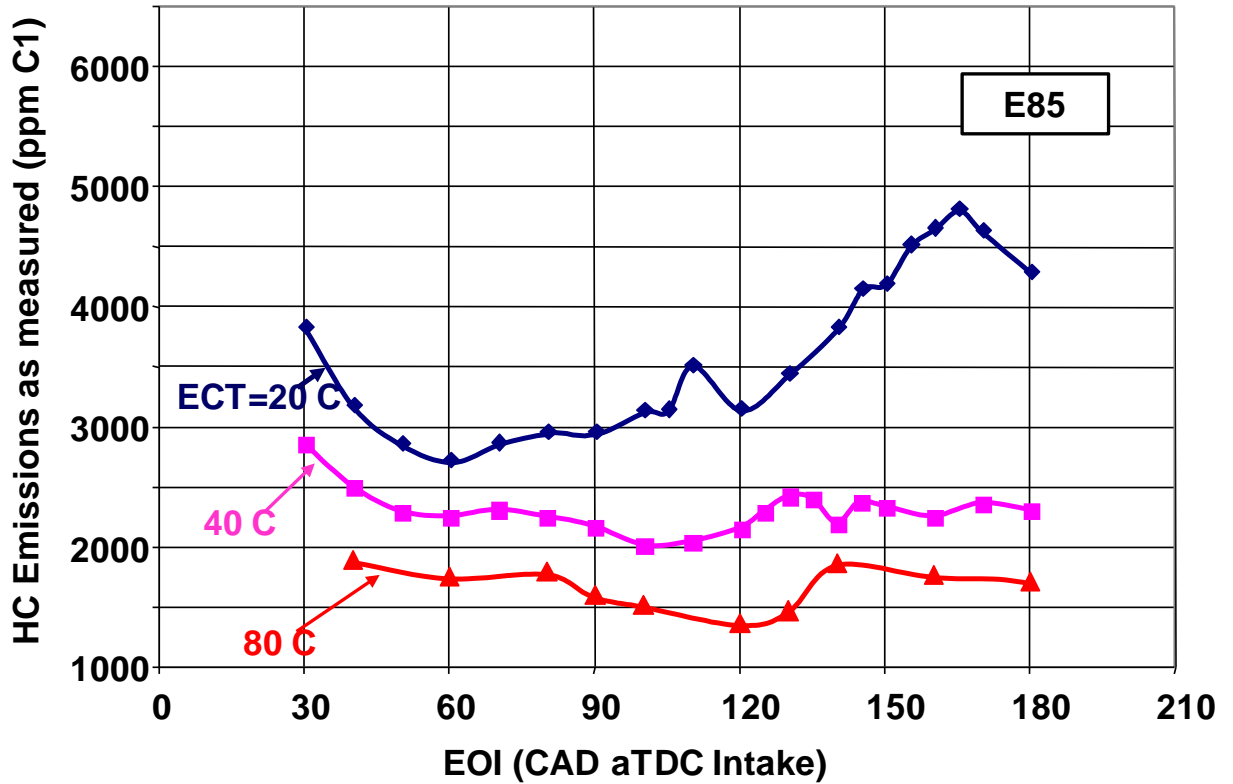


Fig. 24 HC emissions as a function of EOI timing and ECT for E85. Engine at 1200 rpm; $\lambda = 1$; MAP = 0.27 bar (NIMEP \approx 1.5 bar); injection pressure = 70 bar.

The above discussion on the trapping of the un-evaporated fuel in the crevice is also supported by the fuel conversion efficiency data, which are shown in Fig. 25. Here, the fuel conversion efficiency is normalized by the value obtained for E0 at ECT = 80°C. The efficiency decreases with decrease in ECT. For E85, however, there is a further sharp decrease, up to as much as 20% from the reference point, with late injection timing. This decrease may be attributed to the fuel loss to the crevice and the sump.

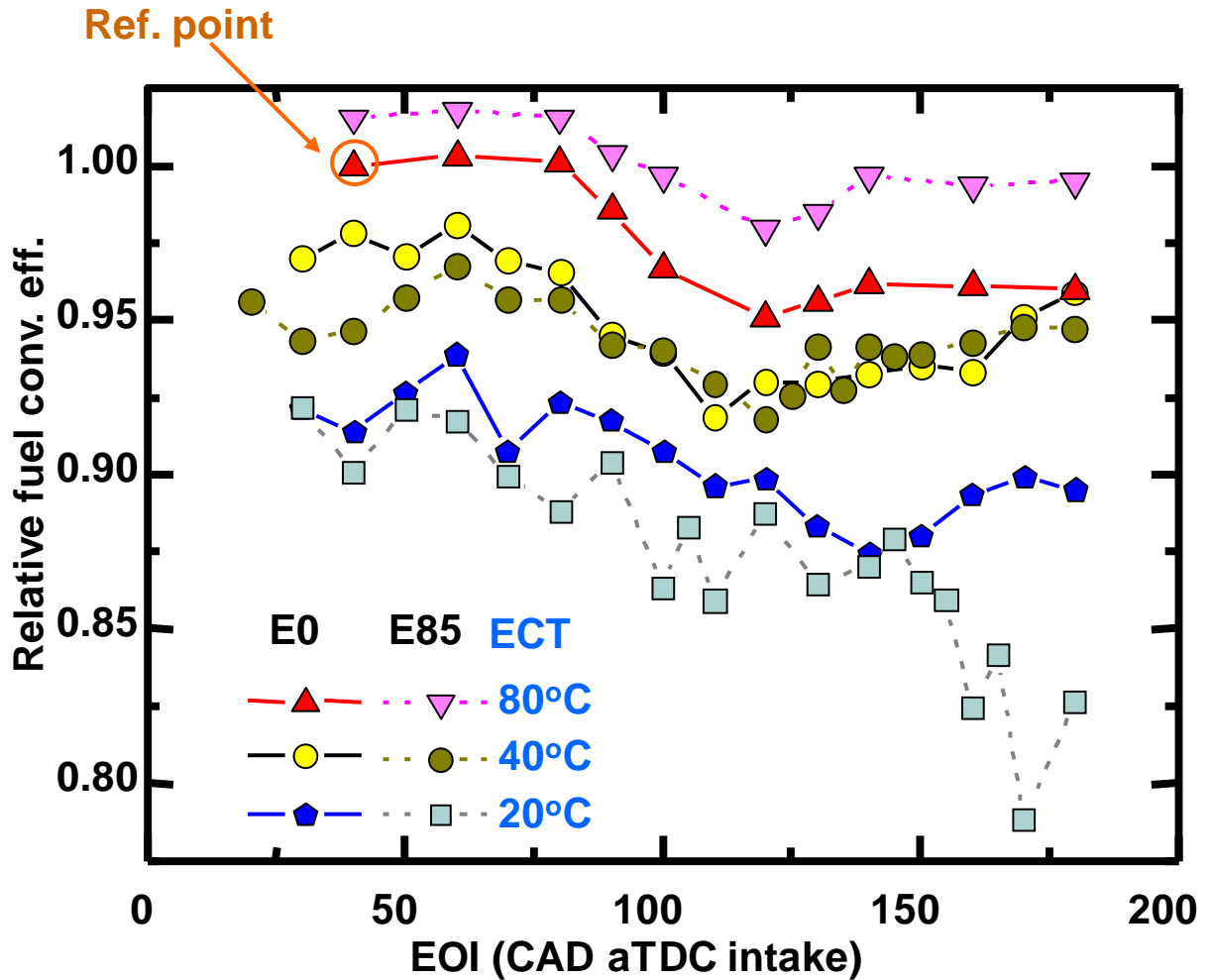


Fig. 25 Fuel conversion efficiency, normalized by the value for E0 at ECT=80°C, for E0 and E85. Engine at 1200 rpm; $\lambda = 1$; MAP = 0.27 bar; injection pressure = 70 bar.

4. SUMMARY AND CONCLUSIONS

The speciated organic gas emissions from a Direct Injection Spark Ignition engine have been assessed with ethanol/gasoline blends of fuels for warmed up moderate load (1500 rpm, 0.38 bar NIMEP, 80°C ECT) and cold fast idle (1200 rpm, 0.15 bar NIMEP, 20°C ECT) conditions. The following observations have been made.

1. The total organic gas emissions (in terms of ppmC1) decrease with increase of ethanol content. Although emissions for the cold engine are substantially higher than the warmed

up one, the slope of the dependence on fuel ethanol content is approximately the same except for E85 at 20° C ECT.

2. The organic gas emissions from E85 at 20° C deviates significantly from the above trend (on the high side). This observation is attributed to the high latent heat of vaporization associated with E85 so that fuel evaporation is suppressed. Substantial liquid fuel may be deposited in the piston crevice and lead to increase in organic gas emissions.
3. For both the warmed up and cold engines, the mole fraction of ethanol in the exhaust is linearly proportional to the liquid volume fraction of ethanol in the fuel (with the exception of E85 at 20° C ECT, as noted above). Every 10 percentage points increase in ethanol content results in 5.5 percentage points increase in exhaust ethanol mole fraction.
4. The molar ratio of ethanol to acetaldehyde in the exhaust is 6 for ethanol/gasoline fuel blends.
5. The mass of a fuel species in the exhaust is proportional to that in the fuel (on a per cycle basis). Thus the exhaust fuel species may be interpreted as a feed-through of the injected fuel species. The feed through rate is higher for the cold than for the warmed up engine. That of the aromatic species is higher than those of the alkanes and ethanol.

The effects of engine operating parameter on the non-speciated HC emissions (as measured by a FID) are also assessed. The following observations are made.

6. Three regimes have been identified in the HC emissions dependence on the injection timing. When injection is early, the emissions are high because the fuel spray bounces off from the piston and liquid fuel is deposited onto the head in the vicinity of the exhaust valve. When injection is at mid stroke, HC emissions are lower, and are relatively insensitive to injection timing. When injection is late, close to the bottom of the stroke,

the HC emissions increases due to the trapping of the fuel in the piston crevice, since the piston comes up almost immediately.

7. The above observation is also found in ethanol gasoline blends at ECT of 20-80° C, except for E85 at 20° C with late injection.
8. For E85 at 20° C with late injection, the high latent heat of vaporization suppresses evaporation. The HC emissions increase significantly; the fuel conversion efficiency also drops. The latter suggests that there is a substantial fuel loss to the crevice and the sump.

ACKNOWLEDGEMENTS

This work was supported by the MIT Consortium for Engine and Fuels Research; the members were Chrysler, Ford, GM, Saudi Aramco, Shell, and VW.

REFERENCES

1. **Iwamoto, Y., Noma, K., Nakayama, O., Yamauchi, T., and Ando, H.** Development of gasoline direct injection engine, SAE technical paper 970541, 1997.
2. **Harada, J, Tomita, T., Mizuno, H., Mashiki, Z., and Ito, Y.** Development of direct injection gasoline engine, SAE technical paper 970540, 1997.
3. **Morita, K., Sonoda, Y., Kawase, T., and Suzuki, H.** Emission reduction of a stoichiometric gasoline direct injection engine, SAE Technical paper 2005-01-3687, 2005.
4. **Davis, R.S., Mandrusiak, G.D., and Landefeld, T.** Development of the combustion system for General Motors' 3.6L DOHC 4V V6 engine with direct injection, SAE Paper 2008-01-0132, 2008.
5. **McNeil, S., Adamovicz, P., and Lieder, F.** Bosch Motronic MED9.6.1 EMS applied on a 3.6L DOHC 4V V6 direct injection engine, SAE paper 2008-01-0133, 2008.

6. **Bandel, W., Fraidl, G. K., Kapus P. E., Sikinger, H., and Cowland, C.N.** The turbocharged GDI engine: boosted synergies for high fuel economy plus ultra-low emission, SAE paper 2006-01-1266, 2006.
7. **Woldring, D., Landenfeld, T., and Christie, R.** DI Boost: application of a high performance gasoline direct injection concept, SAE paper 2007-01-1410, 2007.
8. **Pirelli, M., Di Caprio, F., Torella, E., Mastranelo, G., Pallotti, P., and Marangoni, A.** Fun to drive and fuel economy: the new 1.4 16V turbo gasoline engine from Fiat Powertrain Technologies, SAE paper 2007-24-0062, 2007.
9. **Koga, N., Miyashita, S., Takeda, K., and Imatake, N.** An experimental study on fuel behavior during the cold start period of a Direct Injection Spark Ignition engine, SAE paper 2001-01-0969, 2001.
10. **Francqueville, L. de, Thirouard, B., and Cherel, J.** Investigating unburned hydrocarbon (UHC) emissions in a GDE engine (Homogeneous and Stratified Modes) using formaldehyde LIF and Fast-FID measurements in the exhaust port, SAE paper 2007-01-4029, 2007.
11. **Landenfeld, T., Kufferath, A., and Gerhardt, J.** Gasoline direct injection – SULEV emission concept, SAE paper 2004-01-0041, 2004.
12. **Tsunooka, T., Hosokawa, Y., Utsumi, S. Kawai, T., and Sonoda, Y.** High concentration ethanol effect on SI engine cold startability, SAE paper 2007-01-2036, 2007.
13. **Colpin, C., Leone, T., Lhuillery, M., and Marchal, A.** Key parameters for startability improvement applied to ethanol engines, SAE paper 2009-01-0010, 2009.
14. **Aikawa, K., Sakurai, T., and Hayashi A.** Study of ethanol-blended fuel (E85) effects under cold start conditions, SAE paper 2009-01-0620, 2009.

15. **Voss, E., Schnittger, W., Konigstein, A., Scholten, I., Popperl, ., Pritze, S., Rothenberger, P., Samstag, M.** 2.2 L Ecotec Direct — the new all-aluminum engine with gasoline direct injection for the Opel Signum, 24th Internationales Wiener Enginessymposium, 2003.
16. **Cheng, W.K., Summers, T., and Collings N.** The Fast-Response Flame Ionization Detector. *Prog. Energy Combust. Sci.*, 1998, **24**, 89–124.
17. **Chen, K.C., Cheng, W.K., Van Doren, J.M., Murphy, J.P., Hargus, M.D., and McSweeney, S.A.** Time resolved, speciated emissions from an SI engine during starting and warm-up, SAE paper 961955, 1996.
18. **Kar, K., Cheng, W.K.** Speciated engine-out organic gas emissions from a PFI-SI engine operating on ethanol/gasoline mixtures, SAE paper 2009-01-2673, 2009.
19. **Prostak, A., Lipari, F., and Sigsby, J.E.** Advanced emission speciation methodologies for the Auto/Oil Air Quality Improvement Research Program – I. hydrocarbons and ethers. SAE paper 920320, 1992.
20. **Siegl, W.O., Richert, J.F.O., Trescott, E.J., Schuetzle, D., Swarin, S.J., Loo, J.F., Prostak, A., Nagy, D., and Schlenker, A.M.** Improved emission speciation methodology for Phase II of the Auto/Oil Air Quality Improvement Research Program – hydrocarbons and oxygenates. SAE paper 930142, 1993.
21. **Ekstrom, M., adelsund, K.** Speciation of organic gas emissions from E85 vehicles using mass spectrometry and photoacoustic detection. SAE paper 2009-01-1768, 2009.
22. **Cheng, W.K., Hochgreb, S., Norris, M.G., Wu, K. C.** Auto-Oil Program Phase II Heavy Hydrocarbon Study: Analysis of Engine-Out Hydrocarbon Emissions Data. SAE Transaction, **103**, Sect. 4, Paper 941966, 1994, 1248 - 1263.

23. **Cheng, W.K., Hamrin, D., Heywood, J.B., Hochgreb, S., Min, K.D., and Norris, M.G.**

An Overview of Hydrocarbon Emissions Mechanisms in Spark-Ignition Engines. SAE Transaction, **102**, Paper 932708, 1207-1220, 1993.

24. **Min, K.D., W.K. Cheng.** Oxidation of the Piston Crevice Hydrocarbon During the

Expansion Process in a Spark Ignition Engine. Combust. Sci. and Tech. **106**, 4-6, 307-326, 1995.

NOTATION

AQIRP	Air Quality Improvement Research Program
BDC	Bottom-dead-center
CAD	Crank angle degrees
DISI engine	Direct injection spark ignition engine
E0, E10,...	Ethanol/gasoline blends; the number indicates the volume %
ECT	Engine coolant temperature
EOI	End of injection
EVO, EVC	Exhaust valve open, Exhaust valve close
FID	Flame ionization detector
GC	Gas chromatograph
HC	Hydrocarbon
IVO, IVC	Intake valve open, intake valve close
MAP	Manifold absolute pressure
NIMEP	Net indicated mean effective pressure
PFI	Port-fuel-injection
RI	Retention index
t	Time
TDC	Top dead center
WOT	Wide open throttle